TECHNICAL PAPER

JOURNAL OF THE SOUTH AFRICAN INSTITUTION OF CIVIL ENGINEERING
ISSN 1021-2019
Vol 64 No 2, June 2022, Pages 56–66, Paper 1044

An experimental study of the mechanical behaviour of squat shear walls built with precast concrete two-way hollow slabs

P Luo, J Liu

This paper proposes an innovative precast shear wall system built with precast concrete two-way hollow slabs (PCHS shear walls). In the joints of the precast panels of the PCHS shear walls, noncontact lap splices of rebars with vertical and horizontal holes are used to connect adjacent precast panels. These panels contribute to an automated assembly and facilitate pouring concrete in-situ. The mechanical behaviour of PCHS shear walls and the connection performance of vertical joints are examined through pseudo-static loading testing on one cast-in-situ concrete shear wall and four PCHS shear walls. Moreover, the influences of different parameters, including axial compression ratio, aspect ratio and the magnitude of horizontal distribution reinforcements, were analysed. It was found that the "strong bending and weak shear" requirement was achieved for all specimens. For the PCHS shear walls, the typical prominent diagonal cracks and brittle failure were prevented by the shear slippage at vertical joints and vertical cracks. And the vertical joint enabled the PCHS shear walls to exhibit stable load-bearing capacity with extensive deformations. In addition, the displacement ductility coefficient of all PCHS shear walls was over 5.0, and their ultimate drifts were over 1/100. The bearing capacity was improved with the increase of the axial compression ratio or with the decrease of the aspect ratio, but the deformation capacity was weakened.

PEIYUN LUO is a Lecturer in the Department of Architecture Engineering, Yantai Vocational College, Yantai, China. She received her MS Degree from Yantai University in 2012.

Contact details:
Department of Architecture Engineering
Yantai Vocational College
Yantai 264670
China
E: lpy0902@163.com

JILIANG LIU is a Research Assistant in the School of Civil Engineering, Yantai University, China. He is engaged in the research of fabricated concrete shear wall structures and is the author of many civil engineering publications. He received his MS degree from Yantai University in 2014.

Contact details:
School of Civil Engineering
Yantai University
Yantai 264005
China
E: lianglju@163.com

Keywords: shear wall, precast concrete hollow slab (PCHS), vertical joint, vertical shear crack, load-bearing capacity

INTRODUCTION

There are various types of precast concrete shear walls, of which the connection modes between assembly elements are different. The performance of the joints connecting adjacent precast panels in precast concrete structures is essential to ensure structural integrity. Depending on the construction method, the connection modes can be divided into dry and wet connection modes. The latter mode is suggested for the precast concrete structures in China (MOHURD 2014), because the precast concrete structures connected by wet joints are equivalent to cast-in-situ concrete structures.

The reinforcement connection technology that is the key in the wet connections is divided into direct and indirect connections. The direct connection between different steel bars includes pressed sleeve connection technology (Li *et al* 2016), assembled rebar with lap splice connection technology (Gu *et al* 2019), U-type reinforcement connection technology (Gerber & Van Zijl 2017; Chun & Ha 2015), and annular closed reinforcement anchorage technology (Gholami & Ansari 2018; Zhu & Guo 2018). The indirect connection often refers to the noncontact lap of the rebars, which is connected by cast-in-situ concrete or grout, such as superimposed reinforced concrete walls and shear walls with precast hollow moulds (Chong *et al* 2016; Han *et al* 2019). Note that different studies have demonstrated that direct and indirect connections can transfer stress effectively and ensure the structural integrity of precast concrete shear walls.

A shear wall built with precast concrete two-way hollow slabs (PCHS shear walls) is innovative, in that the reinforcement connection between different assembly units is a noncontact lap. As shown in Figure 1, the connection rebars are set in horizontal and vertical holes of the precast slabs before the concrete is poured. The shear behaviour of PCHS shear walls has been analysed in different studies, which showed that these walls can effectively prevent brittle shear failure, and sustain the vertical and lateral loads at the limit state (Xiong *et al* 2018). Vertical joints are used to connect precast panels in a horizontal direction. Thus, these joints

Luo P, Liu J. An experimental study of the mechanical behaviour of squat shear walls built with precast concrete two-way hollow slabs.
J. S. Afr. Inst. Civ. Eng. 2022:64(2), Art. #1044, 11 pages. http://dx.doi.org/10.17159/2309-8775/2022/v64no2a5

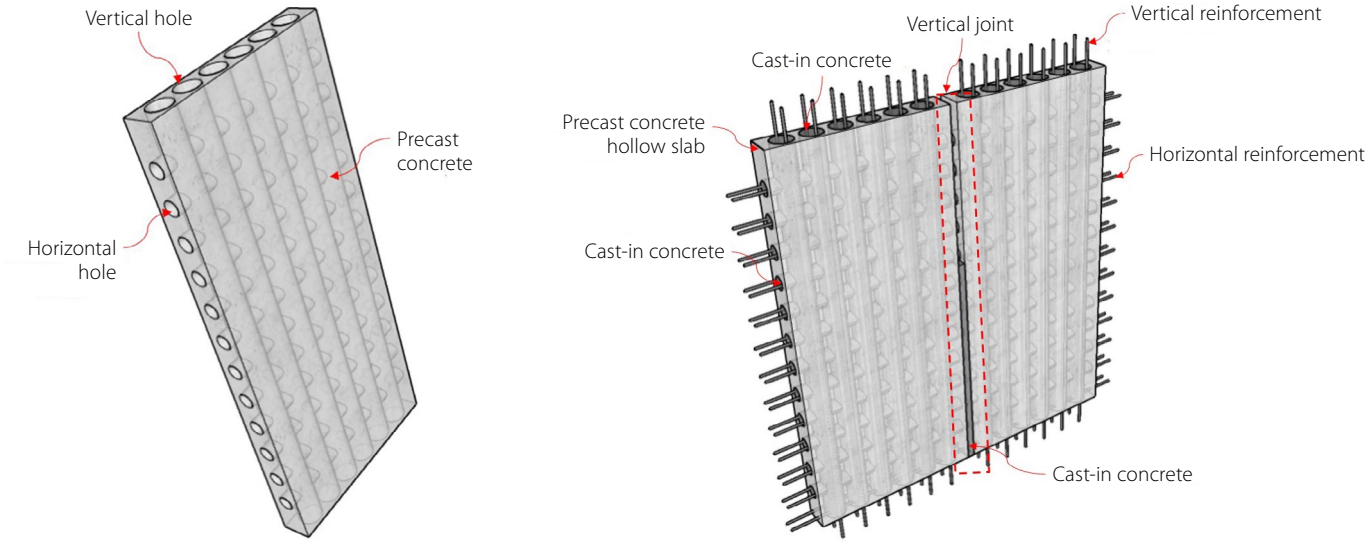

Figure 1 Precast concrete hollow slabs (PCHSs)

are critical sections in a new structure. The joints comprise connection rebars, two old–new concrete interfaces, and cast-in-situ concrete, which is poured in vertical joints and horizontal holes. In this study, to analyse the connection performance of the vertical joints and the shear behaviour of PCHS shear walls, five squat shear wall specimens, comprising one cast-in-situ concrete shear wall and four PCHS shear walls, were designed and tested. Also, the effects of various parameters, including axial compression ratio, aspect ratio, and the magnitude of horizontal distribution reinforcements on the shear behaviour of the specimens, were analysed.

EXPERIMENTAL SETUP

Specimen design

Five shear wall specimens, named SW0, DW1, DW2-N, DW3-L1 and DW5-H, were designed and tested. Specimen SW0 was a contrasting cast-in-situ reinforced concrete (RC) shear wall specimen, and the others were PCHS shear walls. The design details of all these specimens are shown in Figure 2. The width and thickness of the specimens are 1 440 mm and 180 mm, respectively. The height of specimens SW0, DW1, DW2-N and DW5-H is 2 160 mm, and the corresponding aspect ratio is 1.5, while the height of specimen DW3-L1 is 1 440 mm, and the aspect ratio

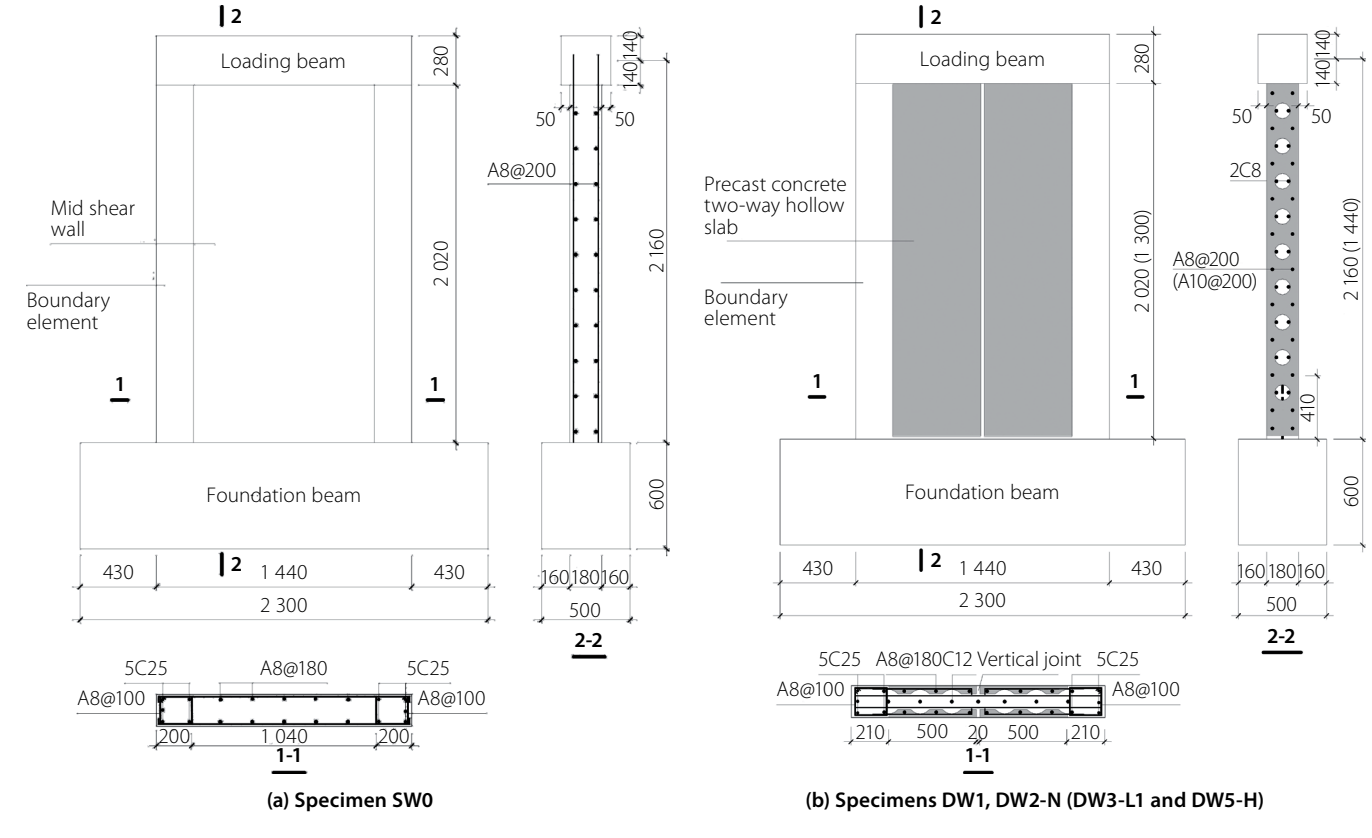

Figure 2 Design detail of specimens (unit: mm)

is 1.0. The dimensions of the loading beam are 1 440 mm (length) × 280 mm (width) × 180 mm (thickness), and the dimensions of the foundation beam are 2 300 mm (length) × 600 mm (width) × 500 mm (thickness).

The cross-section of all specimens consists of two boundary elements and one mid-shear wall. The lengths of the boundary element and the mid-shear wall are 200 mm and 1 040 mm, respectively. For specimen SW0, the mid-shear wall is a cast-in-situ monolithic wall. For PCHS shear walls, the mid-shear walls are composed of two PCHSs, one vertical joint, and cast-in-situ concrete poured in the holes of PCHS and the vertical joint. The width of the PCHS is 500 mm, and that of the vertical joint is 20 mm.

The design principle of all specimens was "strong bending and weak shear" to study the connection behaviour of the vertical joint. The longitudinal reinforcements of each boundary element are 5ϕ25, and the stirrups are ϕ8@100. The vertical and horizontal distribution reinforcements are ϕ8@180 and ϕ8@200, respectively. However, the horizontal distribution reinforcement of DW5-H is ϕ10@200. For PCHS shear walls, the vertical and horizontal distribution reinforcements were arranged in PCHSs. To ensure the connection between two different PCHSs, in each horizontal hole, 2ϕ8 horizontal rebars with both ends anchored into the boundary elements were arranged. The connection between PCHS and the bottom beam depends on the vertical connection rebar ϕ12 anchored in each vertical hole of PCHS. The studied parameters of precast concrete shear wall specimens are axial compression ratio, aspect ratio, and the magnitude of horizontal distribution reinforcements. The axial compression ratios of all specimens can be calculated as $n = N/f_c A$, where N is the axial compressive load, f_c is the concrete compressive strength, and A is the gross cross-section. Note that the axial compression ratio of specimen DW2-N is 0.25, while the axial compression ratio of the other specimens is 0.15.

In actual structures, the vertical joints are used to connect different horizontal PCHSs. To comply with actual engineering conditions, a standard PCHS was averagely cut into two parts. Then they were rotated 180 degrees so that two vertical edges of the standard PCHS were arranged relatively. The cut edge of the PCHSs was roughened, and the horizontal distribution reinforcements were exposed 140 mm, embedded into the edge boundary elements to strengthen the connection between PCHS and the boundary elements. The vertical distribution reinforcements were embedded into the loading beam.

Table 1 Concrete tested strength

Specimens	Concrete strength $f_{cu,m}$ (MPa)			Axial load N (kN)
	Precast	Cast-in-situ	Avg	
SW0	–	32.27	32.27	950
DW1	43.11	35.20	39.16	1 257
DW2-N	43.11	35.20	39.16	1 928
DW3-L1	45.14	37.24	41.19	1 217
DW5-H	43.05	32.27	37.66	1 113

Table 2 Reinforcements tested strength

Type	Grade	$f_{y,m}$ (MPa)	$f_{u,m}$ (MPa)	δ (%)	Functions
A8	HPB300	320	475	27.50	Horizontal and vertical distribution reinforcements of PCHSs
C8	HRB400	417	473	21.25	Stirrups of the boundary elements
C8	HRB400	572	630	17.50	Horizontal connection rebars and vertical and horizontal distribution reinforcements of specimen SW0
A10	HPB300	323	452	22.00	Horizontal distribution reinforcements of specimen DW5-H
C12	HRB400	493	633	26.70	Vertical connection rebar
C25	HRB400	484	623	21.60	Longitudinal reinforcements of boundary elements

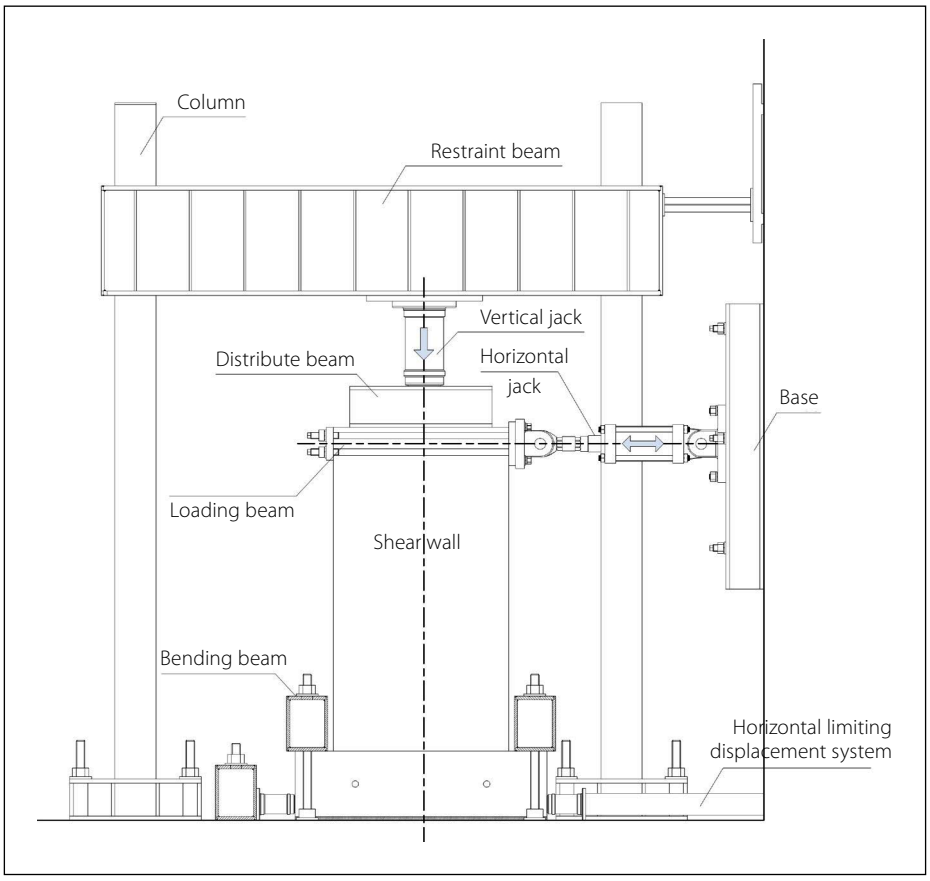

Figure 3 Test set-up

Material properties

The actual cubic compressive strength ($f_{cu,m}$) of concrete was tested on cubes with a size of 150 mm. The results of this test are shown in Table 1. The average concrete cubic compressive strength of each specimen was calculated based on the area ratio of precast or cast-in-situ concrete to the total wall cross-section. The test axial compressive strength of concrete ($f_{c,m}$) was taken as 0.76 $f_{cu,m}$ following GB 50010-2010

(MOHURD 2015), which was used to calculate the axial compression load.

The properties of rebars measured in tension tests are provided in Table 2, where $f_{y,m}$, $f_{u,m}$ and δ denote the measured yield strength, measured tensile strength and percentage of total elongation after fracture, respectively. In Table 2, HPB 300 denotes the hot-rolled plain rebars used in PCHSs, and HRB 400 denotes the hot-rolled ribbed rebars used in other ones.

Loading procedure and arrangement of measuring points

The test set-up is shown in Figure 3, and the lateral loading procedure is shown in Figure 4. First, the constant axial compressive load provided in Table 1 was applied to the loading beam of the specimens and held constant. Then, the cyclic lateral force was applied along the horizontal axis of the loading beam. Based on the elastic-plastic behaviour of ductile structural members, when the load was lower than the yield load, the force control method was used with a single loading cycle at each load level. The load increment was 300 kN for the specimens with an aspect ratio of 1.0, and 250 kN for the specimens with an aspect ratio of 1.5. After the lateral loading force had reached the yield load, the displacement control method with two repeated loading cycles at each displacement

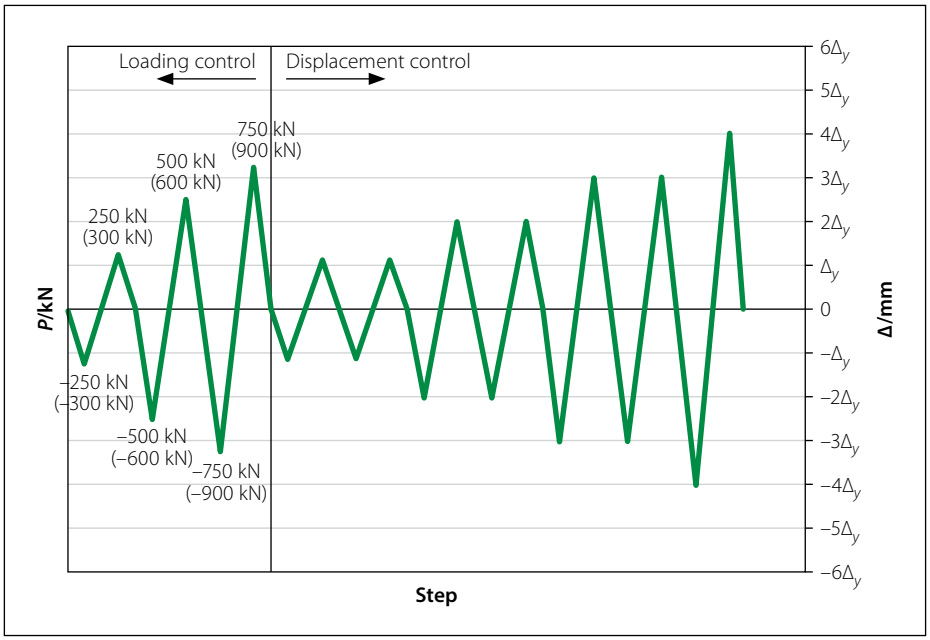

Figure 4 The lateral loading procedure

load level was chosen to investigate the strength degradation and rigidity degradation properties of the specimens. The incremental displacement was Δ_y, which is the horizontal yield displacement observed in the test. When the drift ratio of the specimens reached 1/40, or the lateral bearing capacity was lost, the test was terminated.

Load sensors measured the axial compressive and lateral loads. Also, a displacement gauge (MH1) was positioned in the centre of the top beam to measure the horizontal displacement of the specimen. To obtain the displacement deviation caused by the slippage and the rotation of the bottom beam, a single displacement gauge (BH1) was placed on the horizontal, central axis of the foundation beam. In addition, two displacement gauges (EV5 and WV5) were placed on both sides of the shear walls. Two horizontal relative deformation measuring devices (MH2, MH3) and two vertical

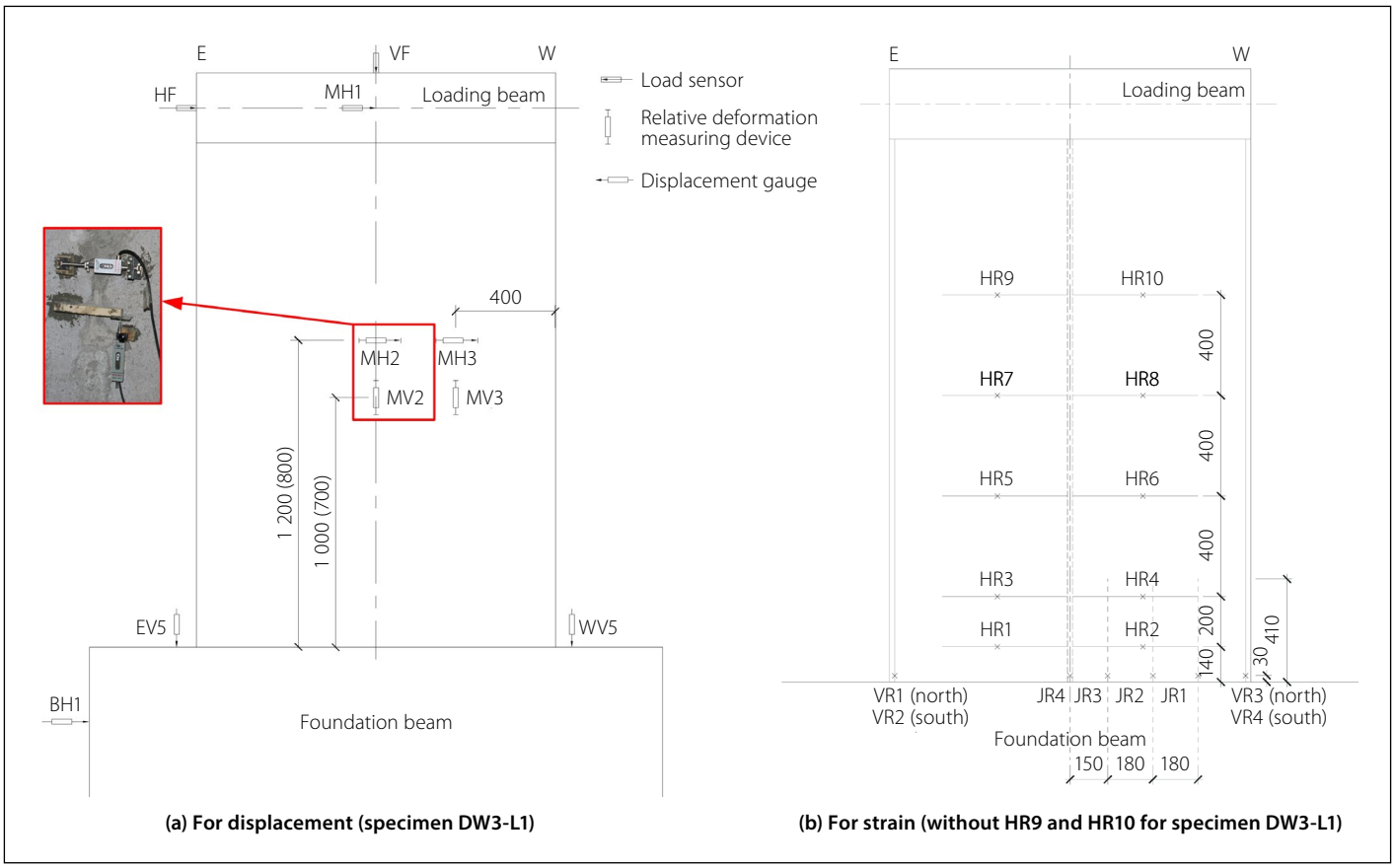

(a) For displacement (specimen DW3-L1)

(b) For strain (without HR9 and HR10 for specimen DW3-L1)

Figure 5 Layout of measurement points of specimens (unit: mm)

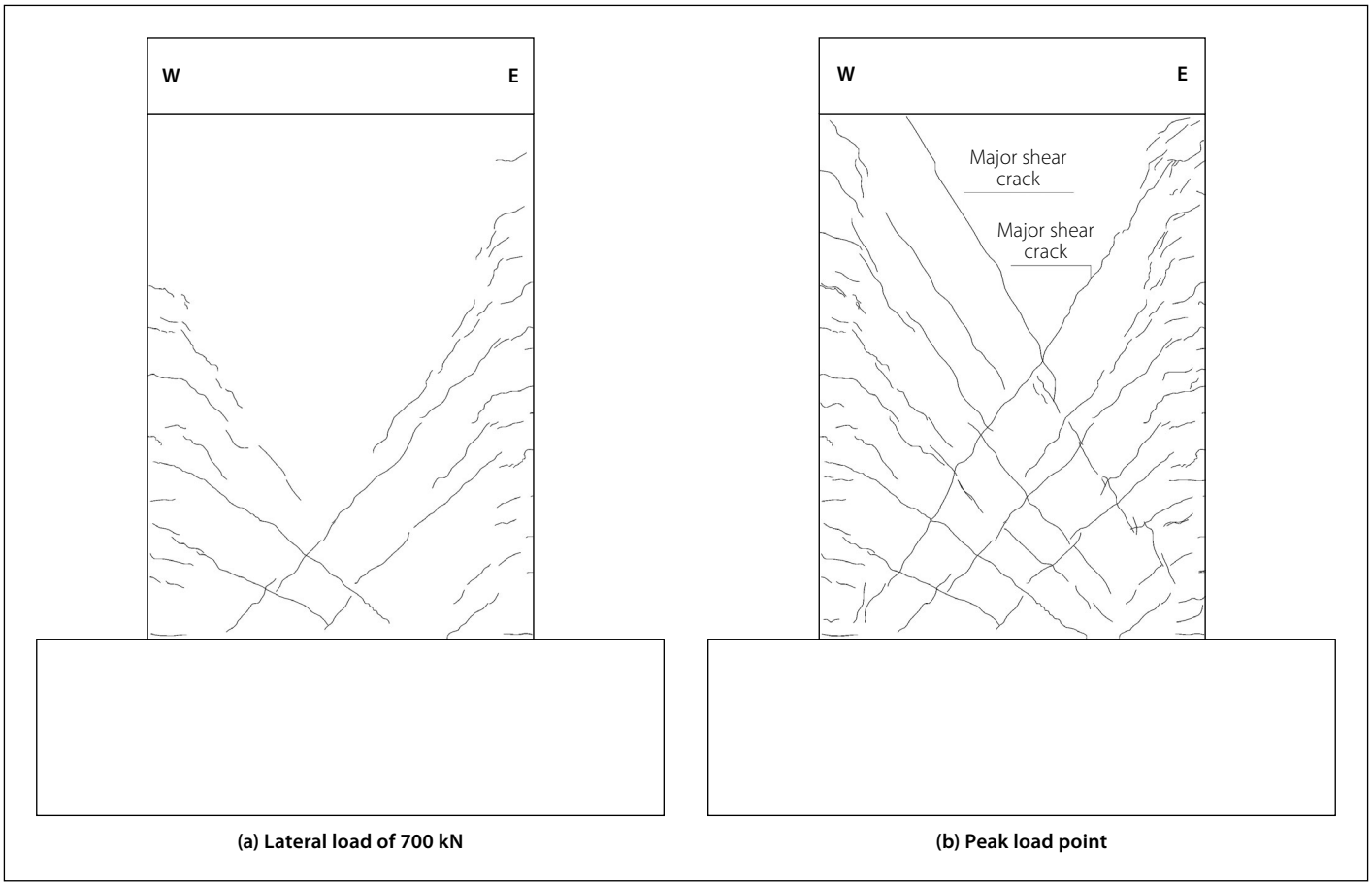

Figure 6 Failure process and pattern of specimen SW0

relative deformation measuring devices (MV1, MV2) were positioned to measure the shear slippage and horizontal opening deformation at the vertical joint and to measure the thickness of the region of the hollow core tubes. Strain gauges were mounted on longitudinal and horizontal rebars to monitor strain responses at different locations, as shown in Figure 5 on page 59.

FAILURE MODES

The failure modes of all specimens were shear failure. However, for PCHS shear walls, a brittle failure did not occur. At peak load, the longitudinal reinforcement of the boundary elements did not yield, while the most horizontal distribution rebars yielded. Also, the root concrete of the boundary elements was not crushed during the test.

Specimen SW0

Figure 6 shows the failure process and pattern of specimen SW0. It is worth mentioning that the positive and negative signs represent pull and push, respectively. Also, a cycle started with a push followed by a pull. When the lateral loads reached –345 and +400 kN, horizontal flexural cracks appeared at the connection between the shear wall and the bottom beam. When the lateral loads were increased to –450 and +530 kN, minor shear cracks with a width less than 0.15 mm occurred. With increasing lateral load, additional horizontal cracks occurred in the boundary elements, which developed into diagonal shear cracks. When the lateral loads were increased to –735 and +861 kN, diagonal tension cracks gradually formed. When the top displacement was controlled at –16.5 mm, the peak strength of –1 015 kN was obtained, and the width of the diagonal tension crack was 2.5 mm. At the next cycle, the width of the diagonal tension crack developed rapidly, and the lateral capacity decreased. Subsequently, the diagonal tension crack propagated throughout the panel, and the axial and lateral strengths decreased abruptly. Then the controlled top displacement reached –22.0 mm, the lateral load declined to around 80% of the peak strength, and the test was over.

Specimen DW1

Figure 7 shows the failure process and pattern of specimen DW1. When the lateral loads reached –310 and +350 kN, horizontal hair-like cracks appeared at the bottom of the specimen. When the drift ratio reached 1/1000, the vertical joint was intact without cracking. When the lateral loads were increased to –376 and +350 kN, some short hair-like inclined cracks appeared at the vertical joint. As shown in Figure 7(a), when the lateral loads reached –550 and +597 kN, inclined shear cracks appeared at the height of 400 – 600 mm from the wall bottom.

With increasing controlled displacement, some short hair-like inclined cracks appeared around the area of vertical core tubes. When the drift ratios reached –1/315 and +1/403, a vertical shear crack region developed along the vertical core tube. Note that this crack region is 400 mm away from the west edge of the wall. Thereafter, three more vertical shear crack regions were formed around the thinnest region of the hollow core tubes. When the drift ratio was +1/138, some horizontal distribution reinforcements yielded, the precast concrete at the vertical shear crack regions spalled slightly, the horizontal opening deformation at the vertical joint increased suddenly, and the specimen reached its peak strength, i.e. +804 kN. The longitudinal reinforcements of the boundary elements were still elastic, and the root concrete was not crushed (Figure 7(b)).

After the peak load point, vertical shear crack regions gradually developed into major vertical cracks, which separated the panel into multiple concrete straps. Thereafter, the load-bearing mechanism of the specimen was transformed from one

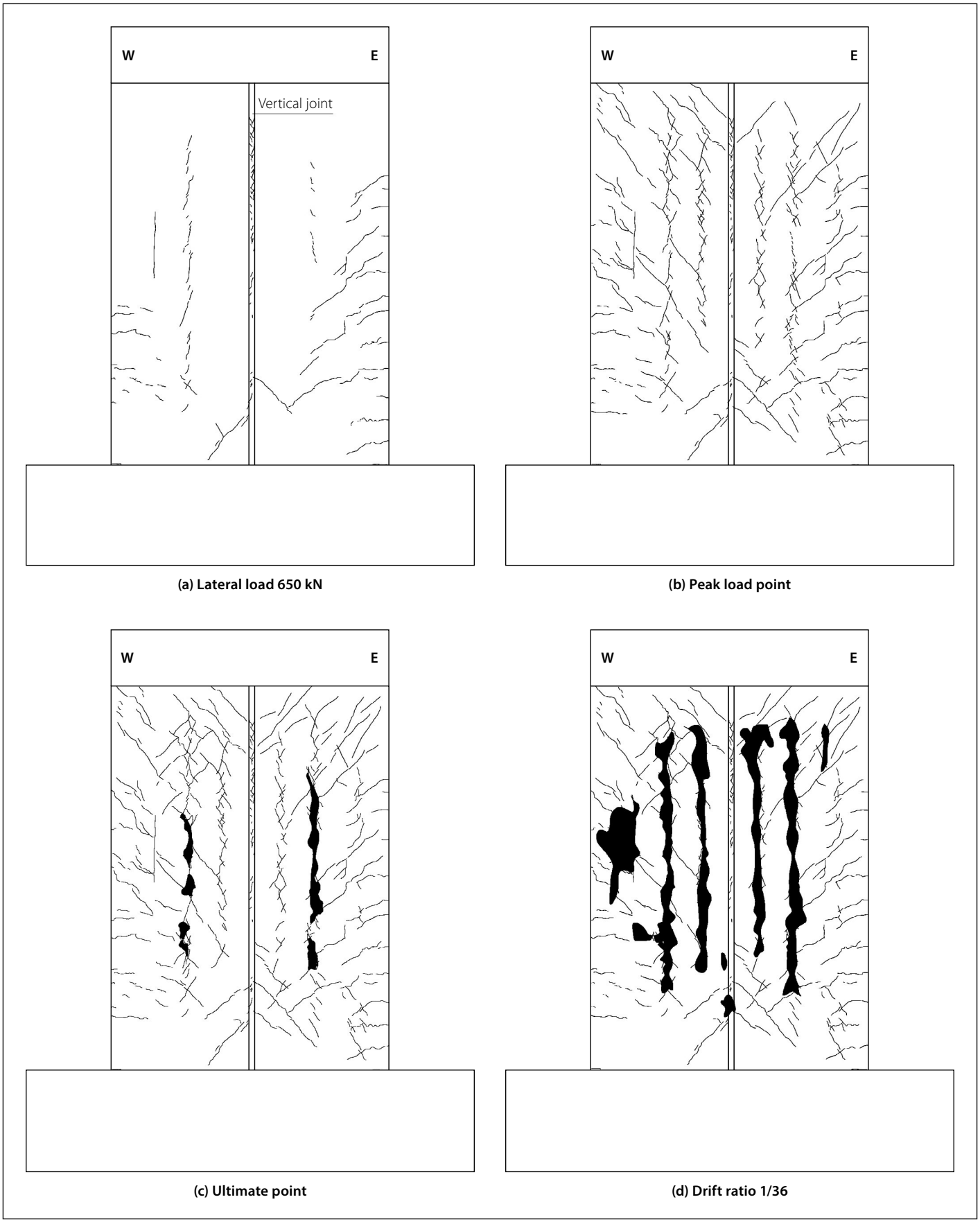

Figure 7 Failure process and pattern of specimen DW1

monolithic panel to a composite system with multiple vertical concrete straps working with horizontal connection reinforcements. As shown in Figure 7(c), when the drift ratio reached 1/72, the ultimate point, in which the strength decreased to 85% of the peak strength, was achieved. Therefore, loading was continued, and more concrete spalling appeared around the major vertical cracks. The loading was terminated when the drift ratio was 1/36. At this point, cast-in-situ concrete in the vertical core tubes was still in good condition. However, as shown in Figure 7(d), severe spalling is found for the precast concrete around the outer parts of the vertical core tubes, while the specimen still maintained an excellent vertical load-bearing capacity.

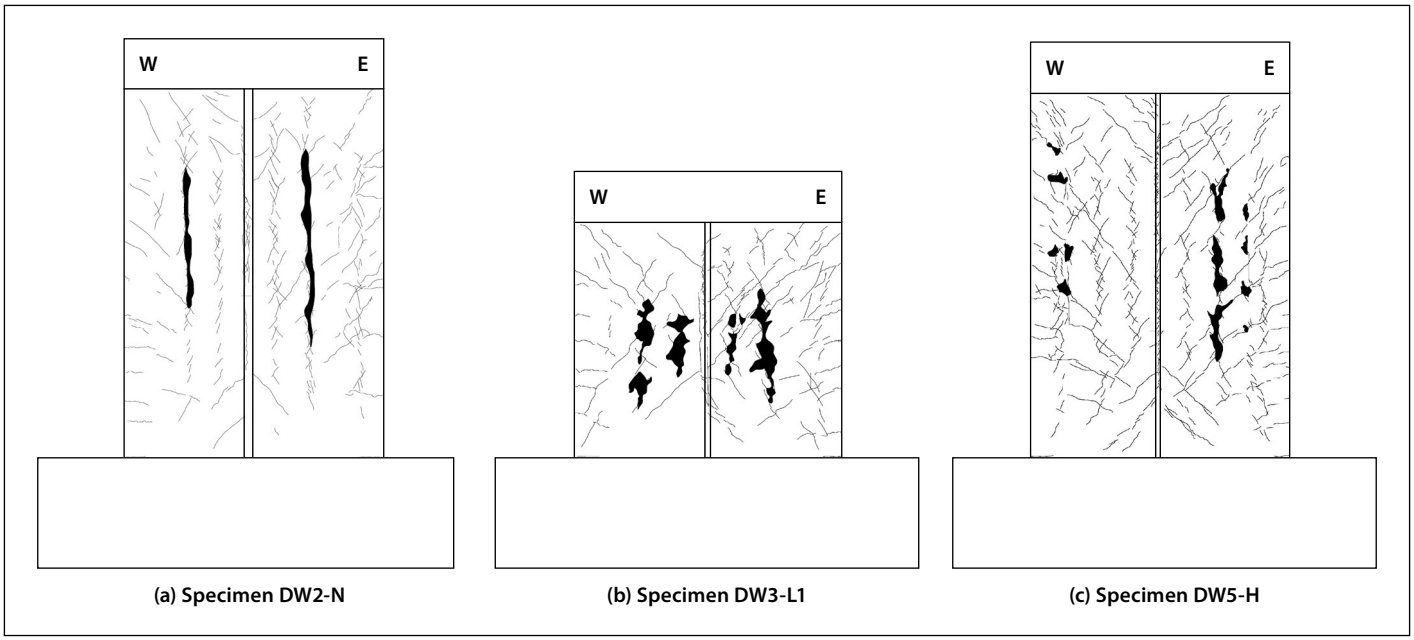

Figure 8 Crack distribution of specimens at the failure point

Specimens with variable parameters

The specimens under the test with variable parameters and at the ultimate point are shown in Figure 8. The axial compressive load of specimen DW2-N is 1 928 kN, and the corresponding axial compression ratio is 0.25, which is different from specimen DW1. When the horizontal hair-like cracks appeared at the bottom of the specimen, the lateral loads were −476 and +468 kN, which were 53.5 and 62.2% higher than for specimen DW1. When short hair-like inclined cracks appeared at the vertical joint, the lateral load of specimen DW2-N increased by 69.9% compared with that of specimen DW1. Also, when the first vertical shear crack region was formed, the lateral load of specimen DW2-N increased by 27.4% compared with that of specimen DW1. Thus, with increasing axial compressive load, the cracking loads of PCHS shear walls increased significantly (Figure 8(a)).

The aspect ratio of specimen DW3-L1 is lower than that of specimen DW1, which is 1.0, while the cracking loads of specimen DW3-L1 are higher. Note that the number of inclined shear cracks of specimen DW3-L1 is more than other specimens. Also, the inclined shear cracks of two different directions intersect, and the precast concrete is cut into diamonds with various sizes. At the peak load point, vertical shear crack regions form at the thinnest region of the hollow core tubes, and minor spalling is also observed. Meanwhile, the horizontal distribution reinforcements yielded. When the drift ratio reached 1/37, the

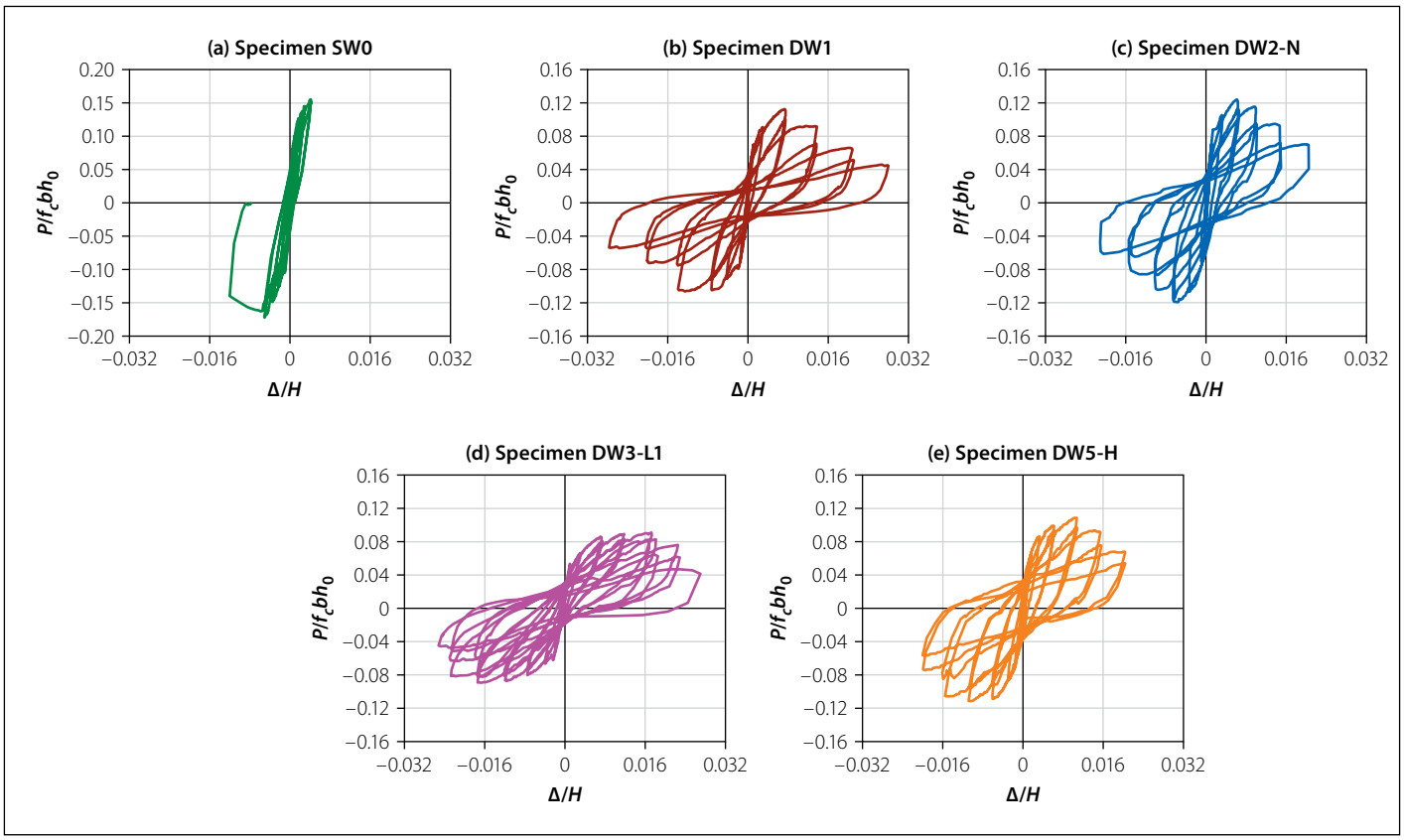

Figure 9 Top lateral force-displacement hysteretic curves of walls

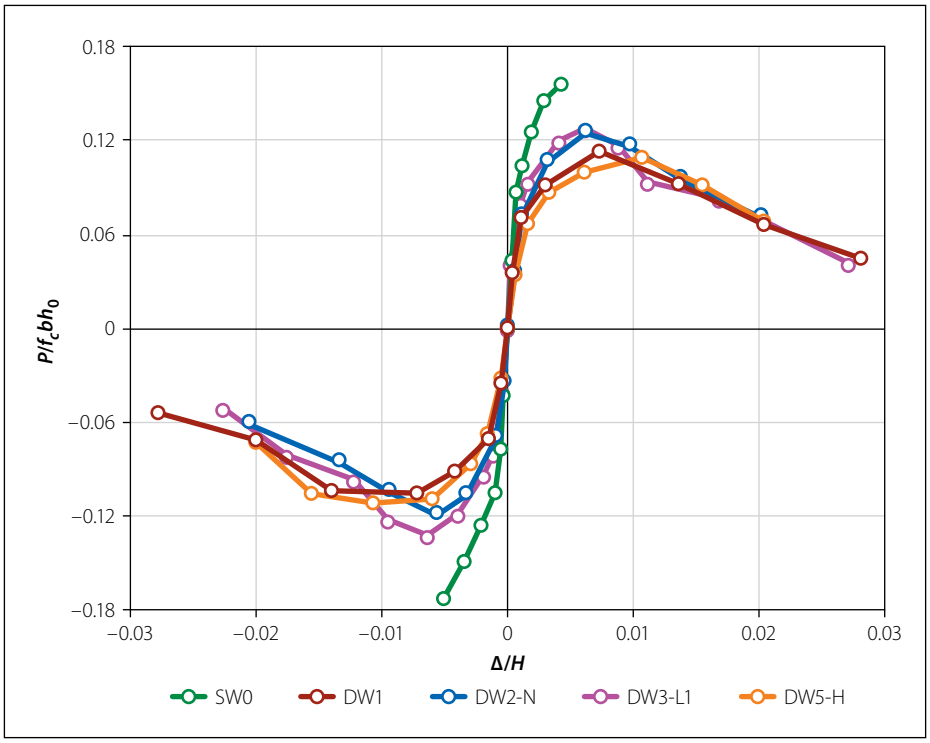

Figure 10 Lateral force-displacement skeleton curves of walls

spalling was serious, while the specimen still maintained an excellent vertical load-bearing capacity, as shown in Figure 8(b).

The horizontal distribution reinforcement of specimen DW5-H is ϕ10@200, and the reinforcement ratio is 56% higher than that of specimen DW1. Note that the crack development process of specimen DW5-H is similar to that of specimen DW1, but the crack width is smaller, as shown in Figure 8(c).

TEST RESULTS

Hysteretic and envelope curves

The lateral force-displacement hysteretic relations at the top sections of the specimens are shown in Figure 9, in which the y-axis is the shear-compression relation, which is used to remove the effect of the concrete strength. Also, the x-axis is the drift ratio (θ), which is the ratio of the lateral displacement to the height of the specimens. Note that the shear-compression relation is calculated as $P/(f_c bh_0)$, where P is the lateral load, b is the width and h_0 is the effective height. Moreover, the effective height is calculated as $h_0 = h\text{-}a_s$, where h is the width of the cross-section and a_s is the distance from the centroid of the longitudinal reinforcements in the boundary element to the corresponding edge of the shear wall. It can be seen that hysteretic curves of PCHS shear walls are much wider than those of the cast-in-situ shear wall SW0. The reason is that the failure mode of specimen SW0 is a brittle shear failure so that the specimen SW0 is broken down after the peak load. It is worth mentioning that the brittle failure of PCHS shear walls is prevented because the vertical shear crack regions form around the thinnest region of the hollow core tubes so that the development path of diagonal tension crack is prevented. For specimen DW2-N, the residual displacement at each load cycle was obviously small, implying low energy dissipation capacity. As the aspect ratio increases, the pinching phenomenon becomes more serious. The cracks of specimen DW5-H developed more thoroughly than the cracks of specimen DW1, and the hysteretic curves of specimen DW5-H are wider.

The envelope curves of the specimens are illustrated in Figure 10. As can be seen, the initial rigidity and maximal force of the cast-in-situ shear wall SW0 are higher than those of specimen DW1, but specimen SW0 has no descending stage. After the peak load point, the lateral force of PCHS shear walls gradually decreases as the horizontal displacement increases. Also, the initial rigidity and the maximal force of specimens DW2-N and DW3-L1 are higher than those of specimen DW1. However, the peak displacements of specimens DW2-N and DW3-L1 are lower, and their descending stages are steeper. In addition, the maximal force increases slightly as the horizontal distribution reinforcements increase.

Loading capacity, deformation and ductility

Note that the main results of all specimens are summarised in Table 3. It should also

Table 3 Characteristics of yield point, peak point and ultimate point

Specimen	Load direction	Effective yield point			Peak point		Ultimate point Δ_u (mm)	Displacement ductility coefficient μ_Δ
		P_y (kN)	Δ_y (mm)	P_m (kN)	$P_m/(f_c bh_0)$	Δ_m (mm)		
SW0	push	724	7.04	1 015	0.164	16.50	16.50	2.38
	pull	685	6.10	915		14.75	14.75	
DW1	push	556	4.78	751	0.109	15.55	36.63	7.34
	pull	574	3.99	804		15.80	27.77	
DW2-N	push	618	3.49	853	0.122	12.20	21.49	4.94
	pull	709	5.73	887		13.41	24.06	
DW3-L1	push	718	2.94	992	0.130	9.18	15.27	6.33
	pull	617	1.64	957		8.90	13.71	
DW5-H	push	629	5.76	838	0.121	23.05	38.17	6.15
	pull	626	6.19	817		23.09	35.32	

be noted that the effective yield point is generated from the envelope curves by the geometric drawing method. Also, the ultimate point is taken as the point corresponding to a 15% reduction in lateral load resistance. In addition, the shear compression ratio $P_m/(f_c bh_0)$ is used to remove the effect of the concrete strength. The displacement ductility coefficient is the ratio of the ultimate displacement (Δ_u) to the yield displacement (Δ_y). According to Table 3, the displacement ductility coefficients of PCHS shear walls are more than or close to 5.0, which are higher than the displacement ductility coefficients of the cast-in-situ shear wall SW0. Also, PCHS shear walls have an excellent deformation capacity.

Compared with the cast-in-situ shear wall SW0, the lateral bearing capacity of specimen DW1 reduces by 33.5%. The reason is that there are some old–new interfaces between the PCHS shear walls and the vertical joint. Also, the relative deformation between the old and new interfaces occurs earlier in the test to affect the integrity of the walls. The effective yield load and the peak load of specimen DW2-N are 17.4 and 11.9% higher than those of specimen DW1. However, the peak displacement and the displacement ductility coefficients are 18.3 and 32.7% lower.

Specimen DW3-L1 has a low aspect ratio equal to 1.0, while its drift ratio at the peak load point is over 1/100. Also, the displacement ductility coefficient of specimen DW3-L1 is 6.33, which is similar to that of specimen DW1. When the aspect ratio of the precast shear wall declines from 1.5 to 1.0, its lateral bearing capacity increases by 19.2%. Also, the effective yield load, effective yield displacement, peak load, peak displacement, and ultimate displacement of specimen DW5-H are all higher than those of specimen DW1. Thus, it can be concluded that, with the increase of the horizontal distribution reinforcements, the mechanical behaviour of PCHS shear walls is improved, even if the horizontal distribution reinforcements are not continuous. The reason is that the development of the vertical shear crack at the thinnest region of the vertical hollow core tubes can be retarded by the horizontal distribution reinforcements.

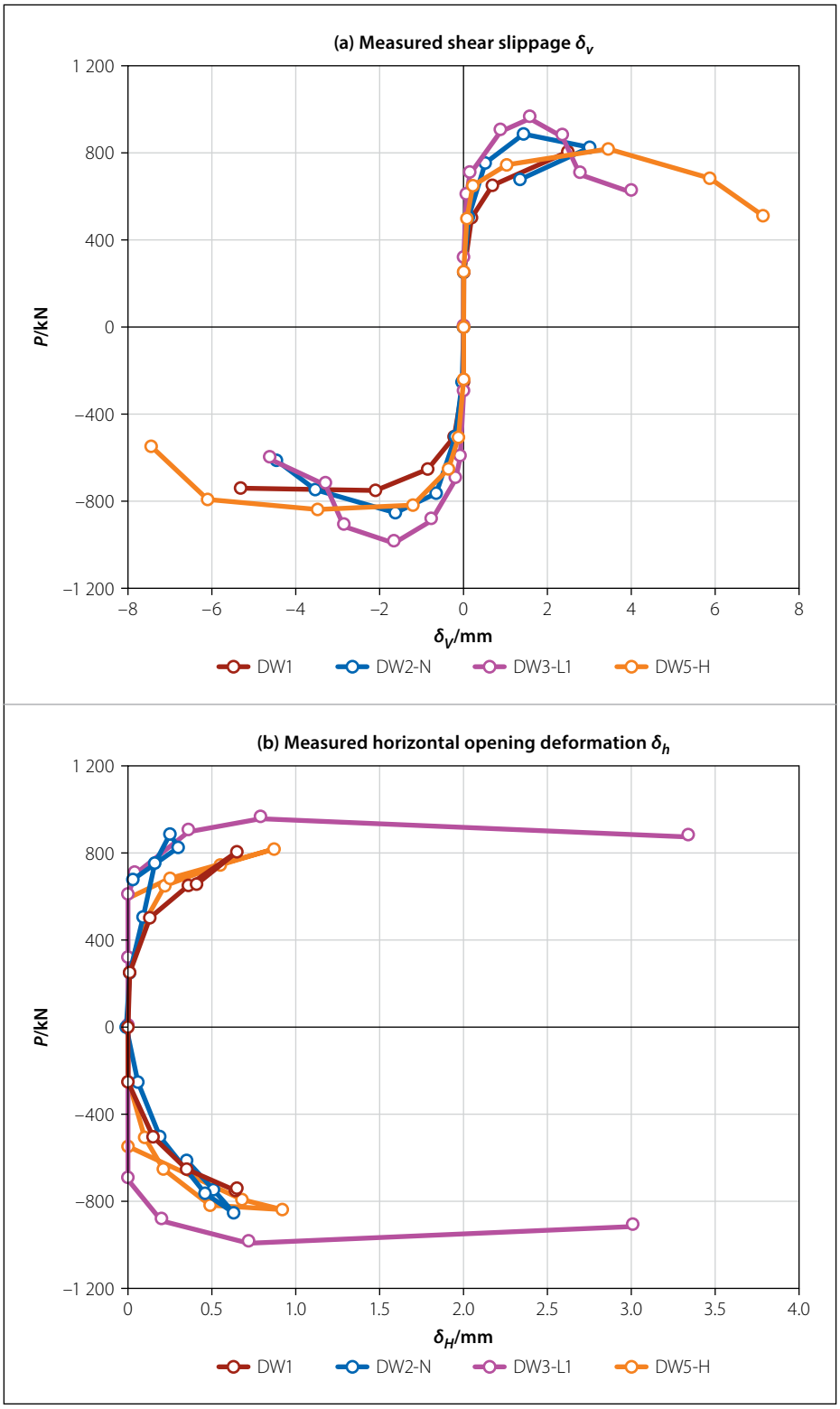

Figure 11 Measured shear slippage (δv) and horizontal opening deformation (δh) at the vertical joints

Shear slippage and horizontal opening deformation

As Figures 11 and 12 illustrate, in precast shear walls the joints that connect PCHSs and internal precast to the cast-in-situ concrete interfaces perform effectively. This is clearly obvious from the shear slippage in vertical joints and vertical shear cracks. Figures 11 and 12 also show that, at the initial stage when the drift ratio is less than 1/600, there is no shear slippage or horizontal opening deformation in the vertical joints and vertical cracks. Thus, it can be concluded that PCHS shear walls are integrated, and the vertical joints can ensure a reliable connection between different PCHSs. Before reaching peak load, there is a slight shear slippage and horizontal opening deformation at the vertical joints. However, no shear slippage and horizontal opening deformation at the vertical shear cracks are found, because the vertical shear cracks at the thinnest region of the vertical hollow core tubes are not formed. Note that, at the peak load, the shear slippage of all PCHS shear walls is 1.58 – 3.48 mm

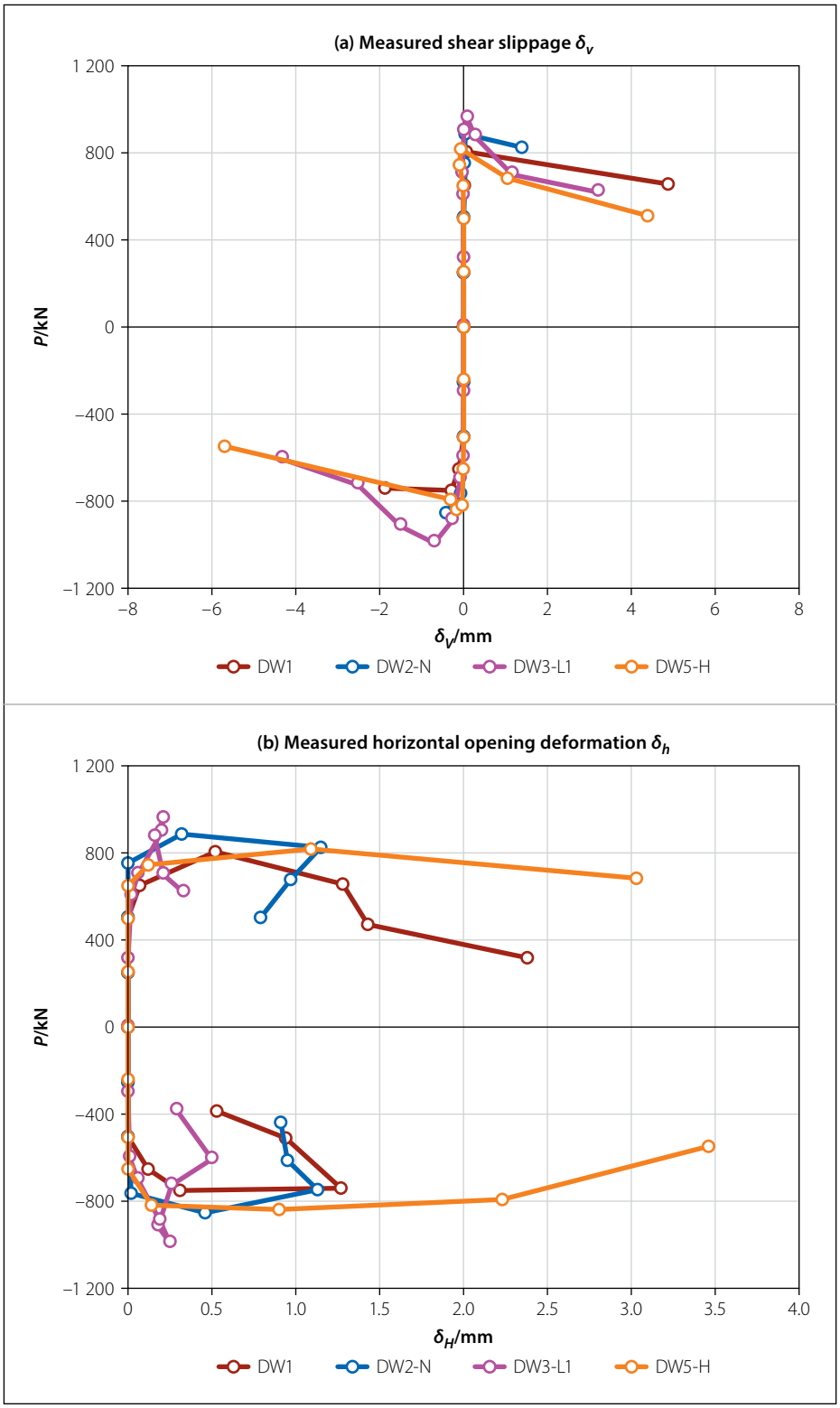

Figure 12 Measured shear slippage (*δv*) and horizontal opening deformation (*δh*) at the vertical shear cracks

and, at the vertical joints, the horizontal opening deformation is 0.23 – 0.92 mm. After the peak load, the vertical shear crack regions gradually developed into major vertical cracks, and the shear slippage and the horizontal opening deformation were generated and increased with increasing controlled displacement. It is worth mentioning that the shear slippage and the horizontal opening deformation at the vertical joints also increased.

The shear slippage and the horizontal opening deformation of the other specimens at the vertical joints are less than those of specimen DW1 under the same lateral load. Thus, with increasing axial compressive ratio and horizontal distribution reinforcements and with decreasing aspect ratio, the shear slippage and the horizontal opening deformation are less. However, there is no specific rule for the vertical shear cracks.

CONCLUSIONS

An innovative precast shear wall system – a shear wall structure that was built with precast concrete two-way hollow slabs (PCHS shear walls) – was proposed in this study. Noncontact lap splices of rebars with vertical and horizontal holes were used in joints to connect adjacent precast panels. The mechanical behaviour of four PCHS shear walls was experimentally analysed and compared with one cast-in-situ shear wall. Also, the connection performance of the vertical joints was studied. The following conclusions can be drawn from the results of this study:

- It was shown that all specimens achieved the desired "strong bending and weak shear" and failed in the shear mode. The failure mode of PCHS shear walls was characterised by plenty of crisscross inclined cracks with a uniform width and vertical cracks along the thinnest region of the hollow core tubes. Shear slippage at vertical joints and vertical cracks prevented the common main diagonal cracks and brittle failure in the cast-in-situ shear wall.
- The bearing capacity of PCHS shear walls was 33.5% less than that of the cast-in-situ shear wall because of the old–new concrete interfaces. However, the deformation capacity was improved significantly. The displacement ductility coefficient reached 7.34, and the ultimate drift was 1/33, which were greater than those of the cast-in-situ shear wall. Thus, PCHS shear walls can be used as primary lateral resistant members in highrise structures.
- The vertical joint in this study was a noncontact lap splice, which contributes to automated assembly and facilitates pouring concrete in-situ. It could enable PCHS shear walls to exhibit stable load-bearing capacity with extensive deformations.
- With increasing axial compression ratio, the bearing capacity increased, but the displacement ductility coefficient, the peak, and the ultimate displacement of the precast shear walls decreased. The aspect ratio had a significant impact on the mechanical behaviour of PCHS shear walls. As the aspect ratio decreased, the bearing capacity increased, and the deformation capacity was weakened. Also, the bearing capacity and the deformation capacity increased with increasing horizontal distribution reinforcements, even if the horizontal distribution reinforcements were discontinuous.

REFERENCES

Chong, X, Xie, L L, Ye, X G, Qing, J & Wang, D C 2016. Experimental study and numerical model calibration of full-scale superimposed reinforced concrete walls with I-shaped cross sections. *Advances in Structural Engineering*, 19(12): 1902–1916.

Chun, S C & Ha, T 2015. Cyclic behavior of wall-slab joints with lap splices of cold-straightened rebars and mechanical splices. *Journal of Structural Engineering*, 141(2): 534–729.

Gerber, J D & Van Zijl, G P A G 2017. Alternative wall-to-slab connection systems in reinforced concrete structures. *Journal of the South African Institution of Civil Engineering*, 59(3): 36–47.

Gholami, R & Ansari, R 2018. Geometrically nonlinear resonance of higher-order shear deformable functionally graded carbon-nanotube-reinforced composite annular sector plates excited by harmonic transverse loading. *European Physical Journal Plus*, 133(2): 56.

Gu, Q, Dong, G, Wang, X, Jang, H B & Peng, S M 2019. Research on pseudo-static cyclic tests of precast concrete shear walls with vertical rebar lapping in grout-filled constrained hole. *Engineering Structures*, 189: 396–410.

Han, W L, Zhao, Z Z, Qian, J R, Zhang Y B & Ma, T 2019. Experimental seismic behavior of squat shear walls with precast concrete hollow moulds. *Earthquake Engineering and Engineering Vibration*, 18(4): 871–886.

Li, N P, Qian, J R, Ye, L P & Liu, S W 2016. Tests on seismic behavior of precast RC shear walls with vertical rebar splicing by pressed sleeve. *Journal of Building Structures*, 37(1): 31–40.

MOHURD (Ministry of Housing and Urban-Rural Development of the People's Republic of China) 2014. *Technical specification for precast concrete structures*. Beijing: China Building Industry Press.

MOHURD 2015. *Code for design of concrete structures*. Beijing: China Architecture & Building Press.

Xiong, C, Chu, M J, Liu, J L & Sun, Z J 2018. Shear behavior of precast concrete wall structure based on two-way hollow-core precast panels. *Engineering Structure*, 176: 74–89.

Zhu, Z F & Guo, Z X 2018. In-plane quasi-static cyclic tests on emulative precast concrete walls. *KSCE Journal of Civil Engineering*, 22(8): 2890–2898.